Switching current of a Cooper pair transistor with tunable Josephson junctions

P. Ågren, J. Walter, and D. B. Haviland
Nanostructure Physics, Stockholm Center for Physics, Astronomy and Biotechnology, Roslagstullsbacken 21, S-106 91 Stockholm, Sweden
(Received 15 January 2002; published 28 June 2002)

We investigate the switching current of a Cooper pair transistor with tunable Josephson energy. The junctions are fabricated in a superconducting quantum interference device (SQUID) geometry which allows for an *in situ* tunable effective Josephson energy by application of a magnetic field. We find a $2e$-periodic switching current versus gate charge. As the magnetic field is increased the switching current stays $2e$-periodic but the magnitude is suppressed. At a magnetic field of half a flux quantum through the SQUID's the switching current is minimum. We can theoretically model the experimental data by assuming a switching current which is proportional to the ideal critical current squarred. We show that such a dependence is expected in the limit where the effect of thermal fluctuations on the system is strong.

DOI: 10.1103/PhysRevB.66.014510 PACS number(s): 74.50.+r, 73.40.Gk, 73.40.Rw

I. INTRODUCTION

Superconducting small capacitance Josephson junction circuits are solid-state electronic systems which exhibit macroscopic quantum mechanical properties. The quantum behavior in such circuits is embodied in the phase number uncertainty relationship for the condensate state of Cooper pairs. The phase and the charge variables are associated to two important energies, the Josephson energy, E_J, and the Coulomb charging energy, E_C. The ratio E_J/E_C together with the electromagnetic environment characterizes the level of phase or charge fluctuations and if Josephson or Coulomb effects are dominating.

One extensively studied system exhibiting such properties is the Cooper pair transistor (CPT).[1–8] The CPT consists of two Josephson junctions in series with a capacitively coupled gate to the central superconducting island. In CPT's the competition between the phase and the charge is typically studied by measuring the maximum supercurrent that can flow through the structure. The maximum supercurrent is controlled by the voltage on the gate. If the parity on the island remains unchanged (i.e., if we can suppress quasiparticle excitations on the island) the maximum supercurrent through the CPT is a $2e$-periodic function of the induced charge on the gate capacitor.

A more direct way of controlling the maximum supercurrent is to replace the two Josephson junctions in the CPT with superconducting quantum interference devices (SQUID's). This enables an *in situ* tuning of the effective Josephson energy of the SQUID's. Harada *et al.*[9] have experimentally investigated this case and they were able to observe a magnetic field tunable supercurrent. However, in their measurement they had a strong effect of quasiparticle poisoning resulting in a weak and only *e*-periodic supercurrent.

We have fabricated CPT's with tunable Josephson energy and measured $2e$-periodic switching currents versus gate potential. Our measurements demonstrate, for the first time, a $2e$-periodic supercurrent as E_J/E_C is continuously varied in the region $2.8 \rightarrow 0$. Although our measurements are free from quasi-particle poisoning and $2e$ periodic in gate charge, excessive thermal fluctuations are necessary to explain the data.

II. THE TUNABLE COOPER PAIR TRANSISTOR

The unbiased tunable CPT with symmetric junctions (see Fig. 1) can be described by the Hamiltonian[7]

$$H = E_C(n - Q_g/e)^2 - 2E_J(\Phi)\cos(\phi/2)\cos(\theta). \qquad (1)$$

The first term is related to the electrostatic energy of the CPT where $E_C = e^2/2C_\Sigma$ is the charging energy of the island, $C_\Sigma \approx 2C_J + C_g$ the total capacitance of the island, n the number of excess Cooper pairs on the island, C_J the capacitance of one SQUID, and $Q_g = C_g V_g$ the gate charge. The second term in the Hamiltonian (1) is due to the Josephson effect and contains the effective Josephson energy for one SQUID, $E_J(\Phi) = E_J^0|\cos(\pi\Phi/\Phi_0)|$, where E_J^0 is the Josephson energy at zero magnetic field, Φ the flux through the SQUID loop and $\Phi_0 = h/2e$ the flux quantum. The sum phase $\phi = \phi_1 + \phi_2$ and the difference phase $\theta = (\phi_2 - \phi_1)/2$ are given in terms of the superconducting phase differences across the Josephson junctions ϕ_1 and ϕ_2. Here n and θ are conjugate variables and ϕ is regarded as a classical variable (see below). The Hamiltonian (1) can easily be diagonalized in a subspace of charge states $|n\rangle$ and used to find the corresponding energy levels $E_m(\phi, Q_g)$, where m is the band index.

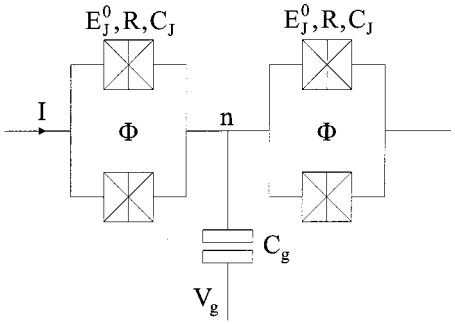

FIG. 1. A schematic picture of the tunable CPT. It consists of two small capacitance SQUID's in series. The island between the two junctions is capacitively connected to a gate electrode which controls the Coulomb blockade of charge tunneling. Here E_J^0, R, and C_J are the Josephson energy at zero magnetic field, the resistance and the capacitance of one SQUID, respectively.

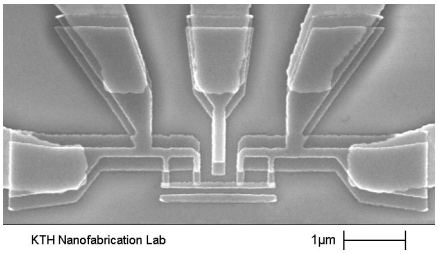

FIG. 2. A scanning electron micrograph of the tunable CPT. The tunable CPT is overlapping to five gold leads.

If a current I is applied to the CPT a term $-(\hbar\phi/2e)I$ is added to the Hamiltonian (1). The external current has the effect of tilting the energy landscape along the ϕ direction, analogous to the tilting of a Josephson washboard potential.[10] The critical current for energy band m for a fixed gate charge Q_g can be found as $I_C^m(Q_g) = (2e/\hbar)\max\{\partial E_m/\partial\phi|_{Q_g}\}$.[5,7]

If there are no unpaired electrons on the island (i.e., we have good control over the quasiparticles) it will have an even parity. In this case the critical current from the lowest energy band is a 2e periodic function of the gate charge with maxima at $Q_g = (e \bmod 2e)$.

The Hamiltonian (1) does not include the electromagnetic environment surrounding the CPT. In reality the environment will have a strong influence on the observable critical current.[11,12] In our measurement the impedance of the environment is determined by the microwave impedance of the measurement leads which typically is of the order of $Z_{\mathrm{env}} \sim Z_0/2\pi \sim 60\Omega$, where Z_0 is the impedance of free space. Thus the impedance of the environment at microwave frequencies is much smaller than the quantum resistance, $\mathrm{Re}[Z_{\mathrm{env}}] \ll R_Q = h/4e^2$. Therefore, quantum fluctuations of ϕ are weak and we regarded it as classical. Thermal fluctuations on the other hand are present in our measurements. In Sec. V we analyze this situation further. We will call the observable (measured) critical current a *switching current*, which is usually different from the ideal theoretical critical current. The switching current is the current at which the measured CPT switches from a near zero voltage to a finite voltage state of order $2\Delta/e$. The switching current is usually smaller than the critical current due to quantum or thermal fluctuations of the phase ϕ.

III. FABRICATION AND MEASUREMENT

Our samples are fabricated using electron beam lithography in two different steps. In the first step we fabricate 2–3 mm long and 40 nm thick gold leads ($\sim$25–50 Ω at 300 K) down to an area of 2×5 $\mu\mathrm{m}^2$. We use normal metal gold leads close to the superconducting structure to trap out-of-equilibrium quasiparticles and prevent them from reaching the CPT island. Experimental evidence for reduced effect of quasi-particle poisoning on CPT's with normal metal leads exists.[4,5] In the second step the mask for the tunable CPT's is defined. The $\mathrm{Al/Al_2O_3/Al}$ CPT's are fabricated using the shadow evaporation technique[13] with thickness 25+25 nm and angle $\pm12°$. To ensure good electrical contact between the gold and the aluminum we expose the developed CPT mask to a light ashing in an oxygen plasma. Figure 2 shows a scanning electron micrograph of the tunable CPT layout.

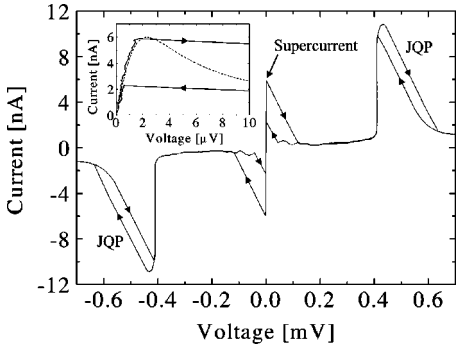

FIG. 3. Current voltage characteristic (IVC) for the tunable CPT at zero magnetic field. The supercurrent and the Josephson Quasiparticle Peaks (JQP) are indicated in the figure. The inset shows a zoom of the low voltage region. A finite voltage supercurrent branch is observed which indicates the effect of phase diffusion. The dashed line is a fit of expression (4).

The samples are measured in an Oxford Instrument Kelvinox AST-minisorb dilution refrigerator with a base temperature of $\sim$35 mK. The measurement leads are filtered at room temperature with RF-feedthrough filters and at the mixing chamber with 1 m of Thermocoax[14] leading to an RF tight can. The sample is mounted in a dual-in-line chip carrier and bonded with aluminum wires.

IV. RESULTS

The current voltage characteristic (IVC) of a tunable CPT is shown in Fig. 3. The normal state resistance R and the island capacitance C_Σ were found from the asymptotic slope and voltage offset in the current-voltage characteristics. For this sample the parameters are $R \approx 8.1$ $k\Omega$ and $C_\Sigma \approx 2.4$ fF, resulting in a Josephson energy $E_J^0 \approx 79$ μeV and a Coulomb energy $E_C \approx 33$ μeV. The IVC shows the supercurrent and the Josephson quasiparticle peak. Also shown in the inset of Fig. 3 is a zoom of the supercurrent region. A clear deviation from a perfect zero voltage supercurrent is observed indicating the presence of noise and the effect of phase diffusion.[15] The current biased IVC is also hysteretic.

Figure 4(a) shows the average switching current versus gate charge as the magnetic field through the SQUID's are changed from 0 G (top) to 80 G (bottom) in steps of 10 G. The switching current is $2e$ periodic and is suppressed to a minimum at a magnetic field of 90 G. This is in good agreement with the estimated field required to minimize the effective Josephson energy: $B_{\min} = \Phi_0/2A \approx 86$ G (where A is the nominal SQUID loop area 400×300 nm^2). If the magnetic field is increased above 90 G the switching current increases again, as the tuning of the switching current is periodic with the flux quanta. The maximum switching current at zero magnetic field is about 6.5 nA. At magnetic fields higher than $\sim$500 G the switching current becomes e periodic.

The switching current data at 0 G show pronounced dips around $Q_g = (e \bmod 2e)$. As the magnetic field is increased towards 90 G the dips gradually disappears. The magnitude

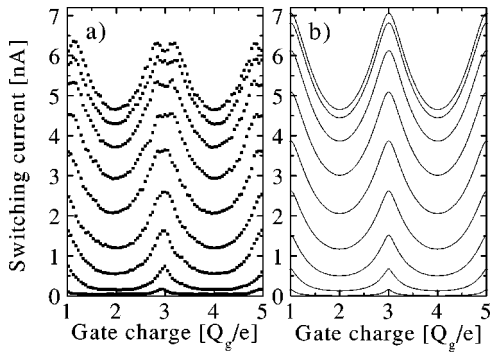

FIG. 4. (a) Switching current of a tunable CPT versus gate charge at different magnetic fields. The magnetic field is changed from 0 G (top) to 80 G (bottom) in steps of 10 G. (b) Modeled switching current. We assume $I_{sw}=aI_C^2$ where I_C is the ideal critical current of a CPT and $a=14.6\times10^6$ A^{-1}.

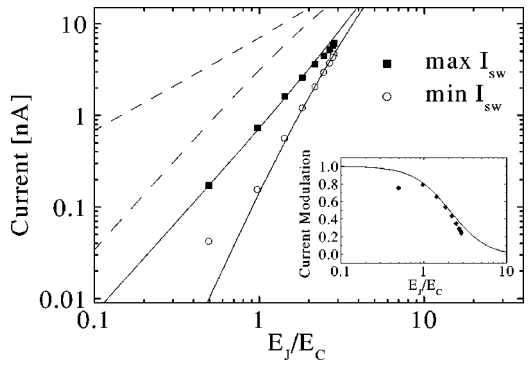

FIG. 5. Comparison between experiment and theory. The scattered data shown the maximum and the minimum switching current as a function of E_J/E_C. The dashed line shows the theoretical critical current and the solid line the modeled switching current using $I_{sw}=aI_C^2$. The inset compares the measured switching current modulation $I_{sw}^{mod}=(I_{sw}^{max}-I_{sw}^{min})/I_{sw}^{max}$ with the modelled switching current modulation assuming $I_{sw}=aI_C^2$.

of the dip feature is periodic with the flux quantum, and is maximized when E_J/E_C is largest. Dips in the switching current are usually caused by either out-of-equilibrium quasiparticles entering the CPT island[4,5,7] or interband transitions.[7,8] We attribute the dips in our measurements to the latter. We rule out out-of-equilibrium quasiparticles as features caused by this mechanism would not disappear as $E_J\rightarrow0$, nor would the dip be periodic in the flux quanta. Interband transitions, on the other hand, can give rise to just such a dependence.

For a symmetric CPT the lowest band ($m=0$) and first excited band ($m=1$) meet at $Q_g=(e \bmod 2e)$ and $\phi=(\pi \bmod 2\pi)$. In the presence of external noise the probability of an interband transition between the lowest and the first excited band is highest at $Q_g=(e \bmod 2e)$. The maximum supercurrent from the first excited band also occurs at $Q_g=(e \bmod 2e)$. At large E_J/E_C the maximum switching current from the first excited band is smaller than the maximum switching current of the lowest band. As $E_J/E_C\rightarrow0$ the maximum switching current from the first excited band approaches the maximum switching current of the lowest band. Thus if interband transitions between the lowest and the first excited band are present, dips would be observed around $Q_g=(e \bmod 2e)$ whose magnitude is large at large E_J/E_C and approaches zero as $E_J/E_C\rightarrow0$.

The maximum switching current at $Q_g=(e \bmod 2e)$ and the minimum switching current at $Q_g=(0 \bmod 2e)$ are plotted versus the E_J/E_C ratio in Fig. 5. Also shown (dashed lines) are the ideal theoretical maximum and minimum critical currents for the CPT. Two observations can be made: (i) the switching current is smaller than the critical current, (ii) the switching current is decreasing more rapidly than the critical current as the E_J/E_C ratio is suppressed. The solid lines in Fig. 5 show a modeled switching current of the form $I_{sw}=aI_C^2$, where a is a constant. This relation between the switching current and the critical current is expected in high effective temperature limit as will be explained in the discussion. With a scaling factor $a=14.6\times10^6$ A^{-1} the model agrees well with the measured switching current over the entire range of E_J/E_C. The deviation between the maximum switching and the maximum critical current at high E_J/E_C ratio is explained by the dip in the maximum switching current at low magnetic fields [Fig. 4(a)]. There is also a deviation between the minimum switching and the minimum critical current at low E_J/E_C ratio. This is due to an experimental problem of measuring low currents.

Using this model, theoretical switching currents versus gate charge can be obtained. Figure 4(b) shows calculated switching currents versus gate charge when we model $I_{sw}=aI_C^2$, where I_C is the ideal critical current calculated from the lowest band. We get a good fit with $E_J/E_C=2.8$, which is 17% larger than estimated from the asymptotic slope and voltage offset in the current-voltage characteristics. Comparison of the Figs. 4(a) and 4(b) shows excellent agreement, with the exception of the interband transition induced dips in the experimental data at large E_J/E_C.

V. DISCUSSION

The above analysis showed that the switching current is scaling as the ideal critical current squarred. To explain this scaling, we view the CPT as an effective Josephson junction with a current-phase relation $I=I_C(Q_g,\Phi)\partial f(\phi,Q_g,\Phi)/\partial\phi$. Here $I_C(Q_g,\Phi)$ is a gate charge and flux-dependent critical current and $f(\phi,Q_g,\Phi)$ a 2π-periodic function in phase ϕ. By using this description it is possible to model the effect of the electromagnetic environment with a simple circuit model. We are using a model that has been used successfully to explain the behavior of a single Josephson junction embedded in a classical electromagnetic environment.[12,15] The circuit is shown in Fig. 6 and consists of a current biased ideal CPT shunted by a capacitor, C_T and a serial combination of a resistor R_n and a capacitor C. This model is the simplest version of a RCSJ model with a frequency-dependent damping which allows the coexistense of both phase diffusion and hysteresis. Here the capacitor $C_T\approx C_J\approx C_\Sigma/2$ describes the capacitance of the CPT. The frequency-dependent shunt R_n and C are describing the external circuit that loads the CPT. In our experiments R_n can be chosen to represent the impedance of

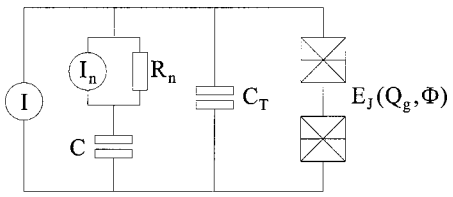

FIG. 6. A simple circuit model for a CPT in an electromagnetic environment. Here $C_T \approx 2C_J$ is the capacitance of the CPT. The frequency-dependent shunt C and R are describing the external circuit that loads the CPT. The CPT is lumped to an effective Josephson junction with a magnetic field and and gate charge dependent Josephson energy $E_J(Q_g,\Phi)$. I_n is the noise current from the resistor R_n.

the measurement leads at microwave frequencies and C a control parameter for the frequency dependence of the impedance.

At high frequencies the external circuit loading the CPT is approximately determined by R. In this limit the system is described by the stochastic differential equation

$$\frac{\hbar}{2e}C_T\ddot{\phi}+\frac{\hbar}{2e}\frac{1}{R_n}\dot{\phi}+I_C(Q_g,\Phi)\frac{\partial f(\phi,Q_g,\Phi)}{\partial\phi}=I+I_n, \tag{2}$$

where I_n is the noise current from the resistor with an autocorrelation $\langle I_n(t)I_n(t+\tau)\rangle=(2k_BT/R_n)\delta(\tau)$.

At microwave frequencies the resistor R_n is of the order of the free space impedance, i.e., $R_n \sim 60\ \Omega$. With a junction capacitance of the order of fF and a junction resistance of the order of $k\Omega$ the CPT is overdamped at these frequencies, i.e., $2\pi^2(R_n/R_Q)^2 \ll E_J/E_C$, where $R_Q=h/4e^2$. In the overdamped limit and if f is a harmonic function of the phase ϕ (e.g., $f=-\cos\phi$ for the single Josephson junction) there exists an analytic solution of the stochastic differential Eq. (2) expressed in terms of modified Bessel functions of complex order[11,16]

$$\frac{I}{I_C(Q_g,\Phi)}=\mathrm{Im}\left[\frac{I_{1-i\alpha v}(\alpha)}{I_{-i\alpha v}(\alpha)}\right], \tag{3}$$

where $\alpha=E_J(Q_g,\Phi)/k_BT$, $E_J(Q_g,\Phi)=I_C(Q_g,\Phi)\hbar/2e$ and $v=V/R_nI_C(Q_g,\Phi)$ is the normalized voltage $V=V_J-R_nI$. In the limit of high temperature ($\alpha<1$) the expression (3) is simplified to

$$I\simeq 2I_m\frac{V/V_m}{(V/V_m)^2+1}, \tag{4}$$

where $I_m=aI_C^2=(\hbar/8ek_BT)I_C^2$ is the maximum supercurrent occuring at a voltage $V_m=(2e/\hbar)k_BTR_n$. If the CPT is viewed as an effective single Josephson junction with harmonic energy bands the switching event is expected to occur at the maximum supercurrent $I_{sw}\simeq I_m=aI_C^2$.

In Sec. IV it was found that a good fit to the measured switching current could be obtained with $a=14.6\times10^6\ \mathrm{A}^{-1}$. By using the expression for $a=\hbar/8ek_BT$ from above we can estimate the effective temperature to $T\approx 400$ mK.

Another way of estimating the effective temperature and also the high frequency impedance of our electromagnetic environment is to fit the expression (4) to the measured IVC at the phase diffusion branch. Such a fit is displayed in the inset of Fig. 3 with dashed lines. The voltage $V_m\approx 2.3\ \mu$V gives an $TR_n\approx 55\ \Omega$K. The maximum supercurrent in this IVC is approximately 6 nA which results in an effective temperature of $T\approx 370$ mK and $R_n\approx 150\ \Omega$. The temperature is in agreement with the estimation above, and the resistance R_n is of the same order as the free space impedance. We attribute the relatively high effective temperature to incomplete filtering of our measurement leads down to the CPT.

VI. SUMMARY

We have investigate the switching current of a CPT with tunable Josephson energy. The junctions are fabricated in a SQUID geometry which enables us to *in situ* tune the effective Josephson energy by application of a magnetic field. We find a $2e$-periodic switching current versus gate charge. As the magnetic field is increased the switching current stays $2e$ periodic and the magnitude is suppressed. This is reported for the first time to the best of our knowledge. Although our measurements are $2e$ periodic we observe a phase diffusion branch and a switching current which is proportional to the ideal critical current squarred. We find that both these observations can be explained by using a simple circuit model where the CPT is shunted with a frequency dependent impedance at an effective temperature. In the overdamped, $2\pi^2(R_n/R_Q)^2 \ll E_J/E_C$, and high effective temperature limit $E_J<k_BT$, thermal noise results in phase diffusion and $I_{sw}\propto I_C^2$. We believe that the high effective temperature is a result of incomplete filtering of our measurement leads.

ACKNOWLEDGMENTS

The authors wish to acknowledge discussions with R. Kautz and support from the EU project SQUBIT, the Swedish NFR, the Wallenberg Foundation and the Göran Gustafsson foundation.

[1] M.T. Tuominen, J.M. Hergenrother, T.S. Tighe, and M. Tinkham, Phys. Rev. Lett. **69**, 1997 (1992).

[2] A. Amar, D. Song, C.J. Lobb, and F.C. Wellstood, Phys. Rev. Lett. **72**, 3234 (1994).

[3] J.G. Lu, J.M. Hergenrother, and M. Tinkham, Phys. Rev. B **57**, 120 (1998).

[4] P. Joyez, P. Lafarge, A. Filipe, D. Esteve, and M.H. Devoret, Phys. Rev. Lett. **72**, 2458 (1994).

[5] P. Joyez, Ph.D. thesis, l'Universite Paris, 1995.
[6] J.G. Lu, J.M. Hergenrother, and M. Tinkham, Phys. Rev. B **53**, 3543 (1996).
[7] D.J. Flees, S. Han, and J.E. Lukens, Phys. Rev. Lett. **78**, 4817 (1997).
[8] D.J. Flees, J.E. Lukens, and S. Han, J. Supercond. **12**, 813 (1999).
[9] Y. Harada, H. Takayanagi, and A.A. Odintsov, Phys. Rev. B **54**, 6608 (1996).
[10] M. Tinkham, *Introduction to Superconductivity*, 2nd ed. (McGraw-Hill, New York, 1996).
[11] G.-L. Ingold, H. Grabert, and U. Eberhardt, Phys. Rev. B **50**, 395 (1994).
[12] P. Joyez, D. Vion, M. Götz, M. Devoret, and D. Esteve, J. Supercond. **12**, 757 (1999).
[13] G.J. Dolan, Appl. Phys. Lett. **31**, 337 (1977).
[14] A. Zorin, Rev. Sci. Instrum. **66**, 4296 (1995).
[15] R.L. Kautz and J.M. Martinis, Phys. Rev. B **42**, 9903 (1990).
[16] Y.M. Ivanchenko and L.A. Zil'berman, Sov. Phys. JETP **28**, 1272 (1969).